



Part 2: Interferometric SAR Time Series for Landslides

Disaster Assessment Using Synthetic Aperture Radar

Eric Jameson Fielding and Alexander Louis Handwerger, Jet Propulsion Laboratory, California Institute of Technology

Oct. 20, 2022

Learning Objectives

By the end of this presentation, you will be able to:

- Understand the basic physics of SAR interferometry
- Describe what SAR interferometric phase tells us about the land surface and landslides
- Describe the necessary data processing for analyzing a time series of SAR interferometry measurements
- Understand the information in SAR interferometric images and time series about land motion



Prerequisites

- ARSET Basics of Synthetic Aperture Radar 2017
- ARSET SAR Processing and Data Analysis 2017
- ARSET Introduction to SAR Interferometry 2017
- ARSET Interferometric SAR for Landslide Observations 2019



Acknowledgments

- Caltech: Z. Yunjun
- JPL: H. Fattahi, N. Pinto, Y. Zheng, P. Agram, E. Gurrola, UAVSAR processing team
- NASA AFRC & JSC: J. McGrath, pilots and staff
- USGS: J. Coe, W. Schulz
- UC Berkeley: R. Bürgmann, B. Delbridge, Xi Hu, Yuankun Liu
- U of Maryland: Mong-Han Huang
- NASA Earth Surface and Interior, Geodetic Imaging, NISAR Science Team programs





SAR Interferometry Theory (Review)

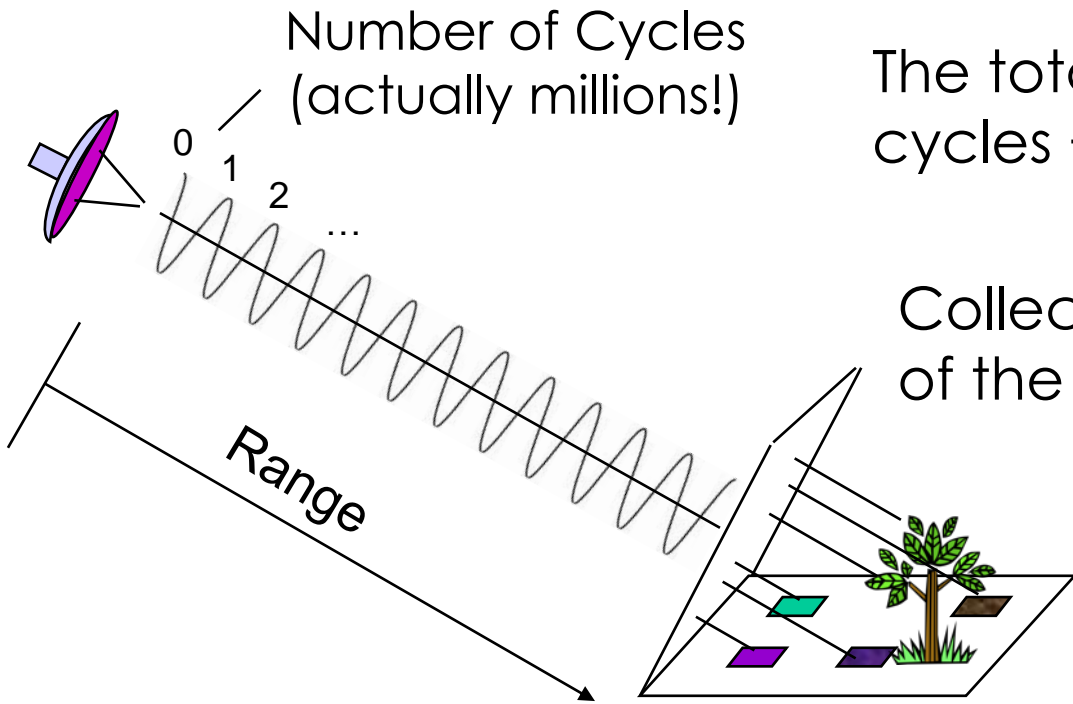
SAR Interferometry Theory

- Quick review of synthetic aperture radar interferometry theory.
- See the 2017 ARSET training “Introduction to SAR Interferometry” and 2019 ARSET training “Interferometric SAR for Landslide Observations” for more details.
- In SAR interferometry, it is all about the phase of the SAR signal.



SAR Phase – A Measure of the Range and Surface Complexity

The phase of the radar signal is the number of *cycles of oscillation* that the wave executes between the radar and the surface and back again.



The total phase is a two-way range measured in wave cycles + random components from the surface.

Collection of random path lengths jumbles the phase of the echo.

Only *interferometry* can sort it out!

Slide modified from Paul Rosen (JPL)

A Simplistic View of SAR Phases

Phase of Image 1 $\phi_1 = \frac{4\pi}{\lambda} \cdot \rho_1 + \text{other constants} + n_1$

Phase of Image 2 $\phi_2 = \frac{4\pi}{\lambda} \cdot \rho_2 + \text{other constants} + n_2$

1. The “other constants” cannot be directly determined.
2. “Other constants” depends on scatterer distribution in the resolution cell, which is unknown and varies from cell to cell.
3. The only way of observing the range change is through interferometry (cancellation of “other constants”).



SAR Interferometry Applications–Mapping

- Mapping/Cartography
 - SAR interferometry was used for the 2000 Shuttle Radar Topography Mission (SRTM), new 2018 release as NASADEM.
 - Radar Interferometry from airborne platforms is routinely used to produce topographic maps as digital elevation models (DEMs).
 - 2–5 meter circular position accuracy
 - 5–10 m post spacing and resolution
 - 10 km by 80 km DEMs produced in 1 hr on a mini-supercomputer
 - NASA SAR topography presently acquired by GLISTIN
 - Radar imagery is automatically geocoded, becoming easily combined with other (multispectral) data sets.
 - Applications of topography enabled by interferometric rapid mapping
 - Land use management, classification, hazard assessment, intelligence, urban planning, short and long time scale geology, hydrology.

Slide modified from Paul Rosen (JPL)



SAR Interferometry Applications–Changes

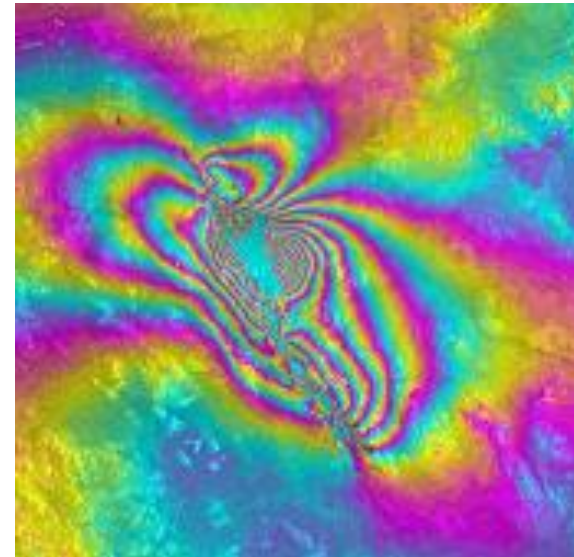
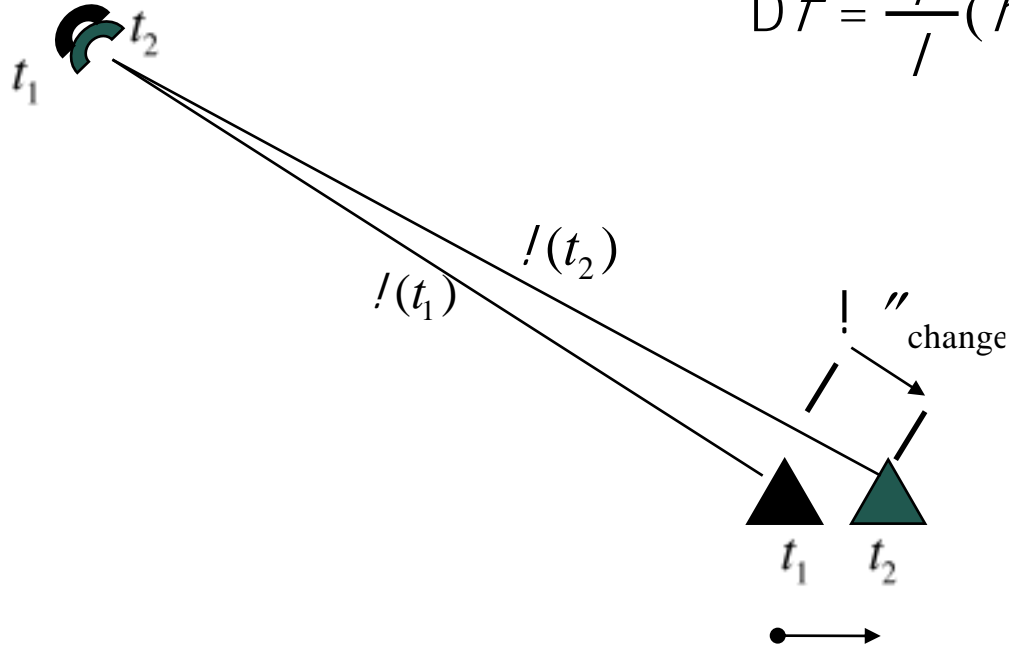
- Deformation Mapping and Change Detection
 - Repeat-pass radar interferometry from spaceborne platforms is routinely used to produce surface change maps as digital displacement models (DDMs).
 - 0.1–1 centimeter relative displacement accuracy
 - 10–100 m post spacing and resolution
 - 10–350 km wide DDMs produced rapidly once data is available
 - Applications include
 - Earthquake and volcano monitoring and modeling
 - Landslides and ground subsidence
 - Glacier and ice sheet dynamics
 - Deforestation, change detection, disaster monitoring



Differential Interferometry

- When two observations are made from the same location in space but at different times, the interferometric phase is proportional to any change in the range or distance of a surface feature directly.

$$\Delta f = \frac{4\rho}{\lambda} (r(t_1) - r(t_2)) = \frac{4\rho}{\lambda} \Delta r_{\text{change}}$$



Slide modified from Paul Rosen (JPL)



Differential Interferometry Sensitivities

- The reason differential interferometry can detect millimeter-level surface deformation is that the differential phase is much more sensitive to displacements than to topography.

$$\begin{aligned} \frac{\partial \phi}{\partial h} &= \frac{2\pi \rho b \cos(\theta - \alpha)}{\lambda \rho \sin \theta} = \frac{2\pi \rho b_{\perp}}{\lambda \rho \sin \theta} && \text{Topographic Sensitivity} \\ (\phi \Leftrightarrow \Delta\phi) \quad \frac{\partial \phi}{\partial \Delta\rho} &= \frac{4\pi}{\lambda} && \text{Displacement Sensitivity} \\ \sigma_{\phi_{topo}} &= \frac{\partial \phi}{\partial h} \sigma_h = \frac{4\pi}{\lambda} \frac{b_{\perp}}{\rho \sin \theta} \sigma_h && \text{Topographic Sensitivity Term} \\ \sigma_{\phi_{disp}} &= \frac{\partial \phi}{\partial \Delta\rho} \sigma_{\Delta\rho} = \frac{4\pi}{\lambda} \sigma_{\Delta\rho} && \text{Displacement Sensitivity Term} \\ \text{Since } \frac{b}{\rho} &\ll 1 \quad \Rightarrow \quad \frac{\sigma_{\phi_{disp}}}{\sigma_{\Delta\rho}} \gg \frac{\sigma_{\phi_{topo}}}{\sigma_h} \end{aligned}$$

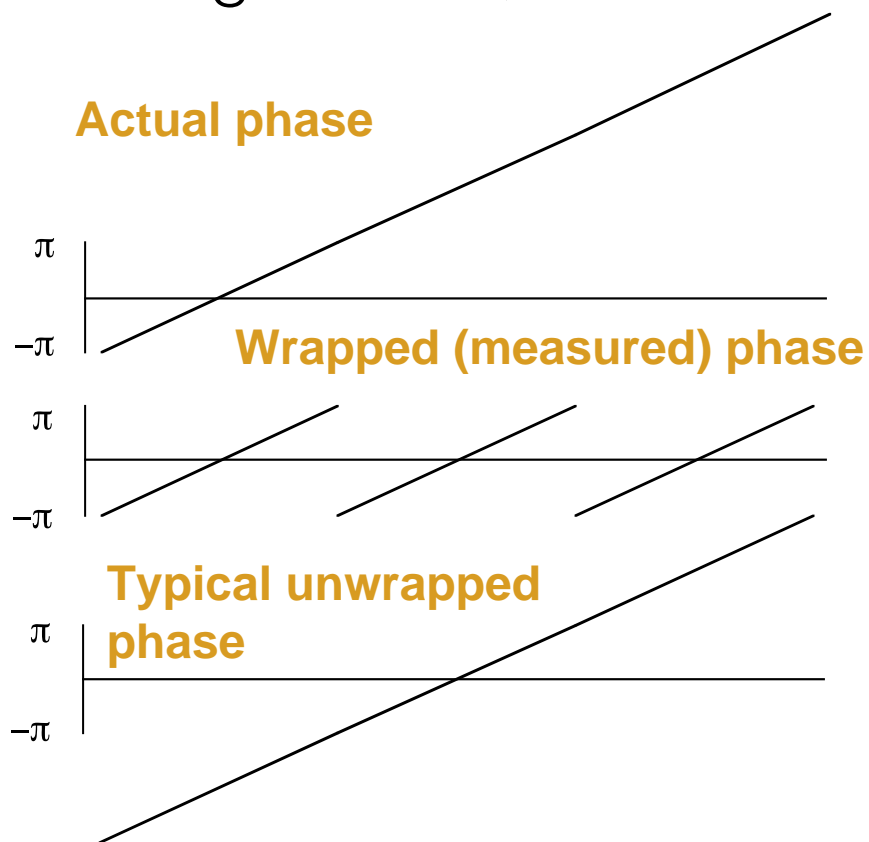
Meter Scale Topography Measurement - Millimeter Scale Topographic Change

Slide modified from Paul Rosen (JPL)



Phase Unwrapping

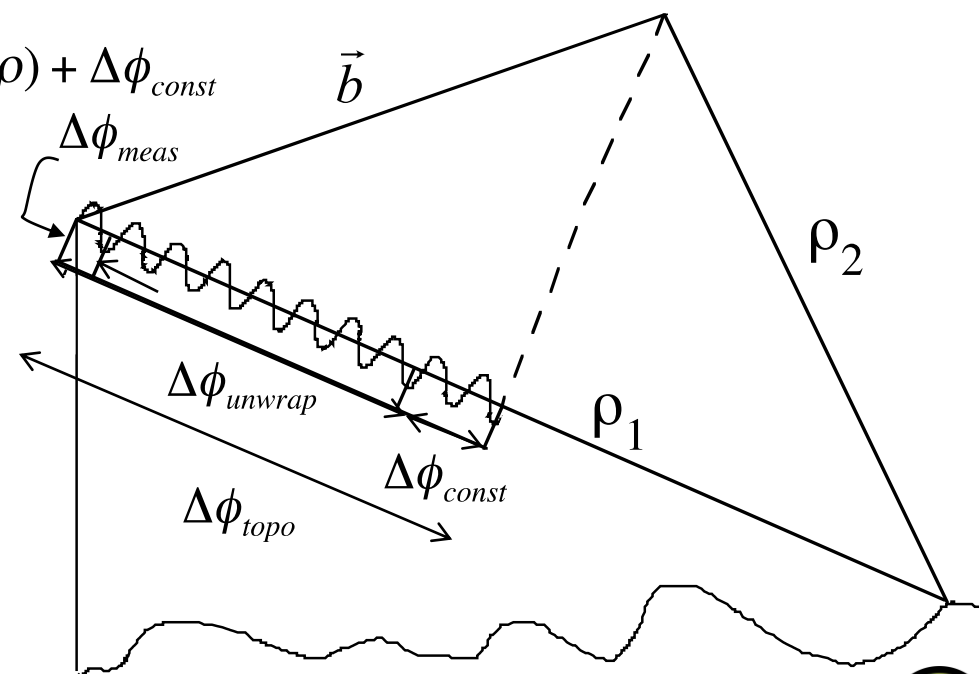
- From the measured, wrapped phase, unwrap the phase from some arbitrary starting location, then determine the proper 2-pi phase “ambiguity.”



$$\Delta\phi_{topo} = \frac{2\pi\rho}{\lambda}(\rho_1 - \rho_2) = \frac{2\pi\rho}{\lambda}\vec{b} \cdot \vec{l}$$

$$\Delta\phi_{meas} = \text{mod}(\Delta\phi_{topo}, 2\pi)$$

$$\Delta\phi_{unwrap}(s, \rho) = \Delta\phi_{topo}(s, \rho) + \Delta\phi_{const}$$



Slide modified from Paul Rosen (JPL)



Correlation* Theory

- InSAR signals decorrelate (become incoherent) due to
 - Thermal and Processor Noise
 - Differential Geometric and Volumetric Scattering
 - Rotation of Viewing Geometry
 - Random Motions Over Time
- Decorrelation relates to the local phase standard deviation of the interferogram phase.
 - Affects height and displacement accuracy
 - Affects ability to unwrap phase

*“Correlation” and “Coherence” are often used synonymously

Slide modified from Paul Rosen (JPL)



InSAR Correlation Components

- Correlation effects multiply, unlike phase effects that add.
- Low coherence or decorrelation for any reason causes loss of information in that area.

$$\gamma = \gamma_v \gamma_g \gamma_t \gamma_c$$

where

γ_v is volumetric (trees)

γ_g is geometric (steep slopes)

γ_t is temporal (gradual changes)

γ_c is sudden changes



Wavelength: A Measure of Surface Scale

Light interacts most strongly with objects around the size of the wavelength.

L (24 cm)

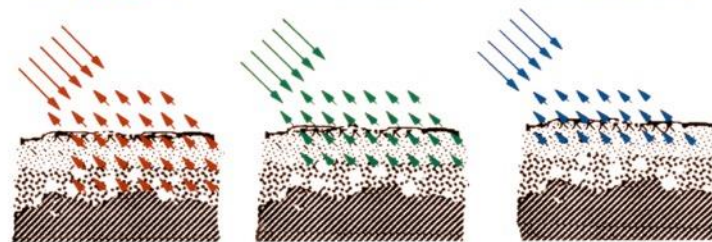
C (6 cm)

X (3 cm)

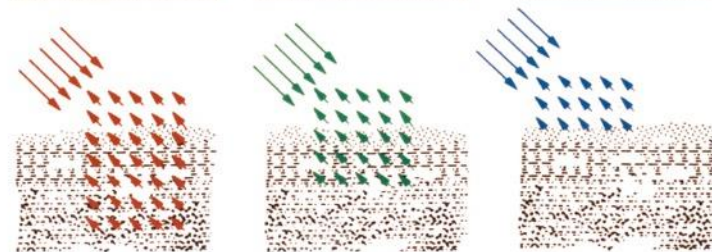
Forest: Leaves reflect X-band wavelengths but not L-band



Dry Soils: Surface looks rough to X-band but not L-band



Ice: Surface and layering look rough to X-band but not L-band



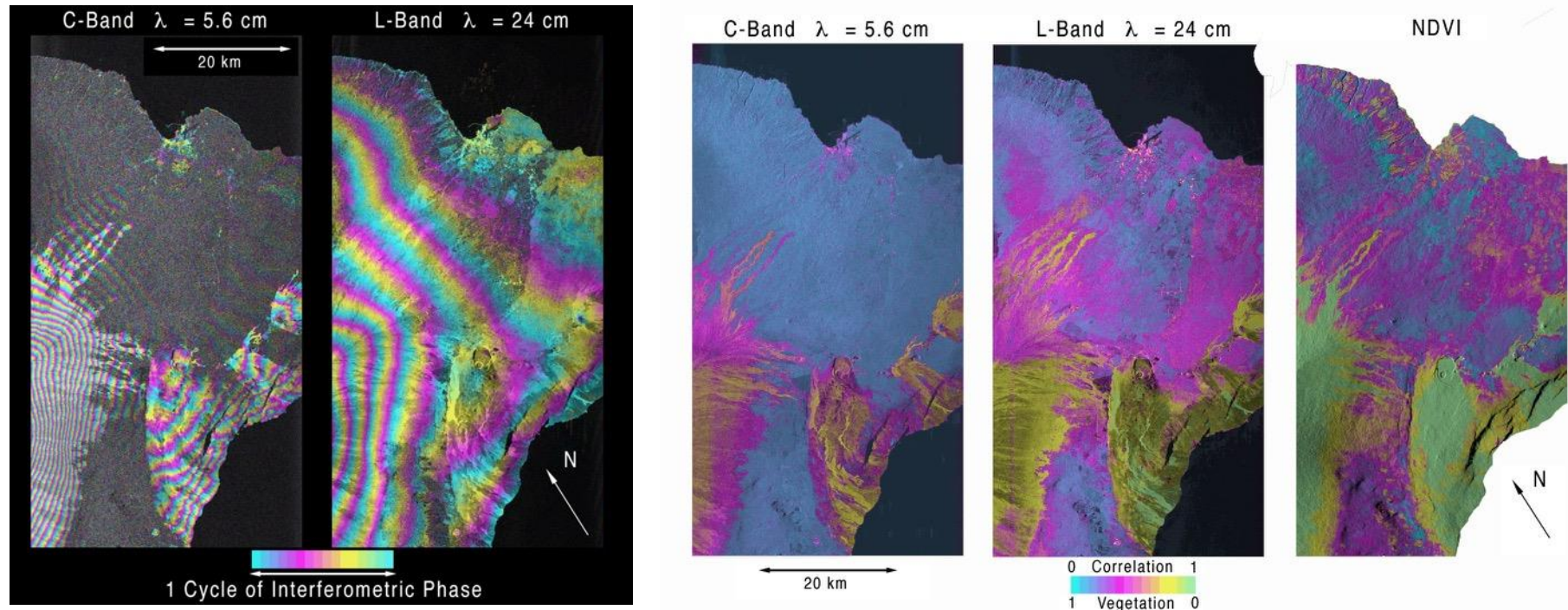
Slide modified from Paul Rosen (JPL)



InSAR Coherence and Wavelength

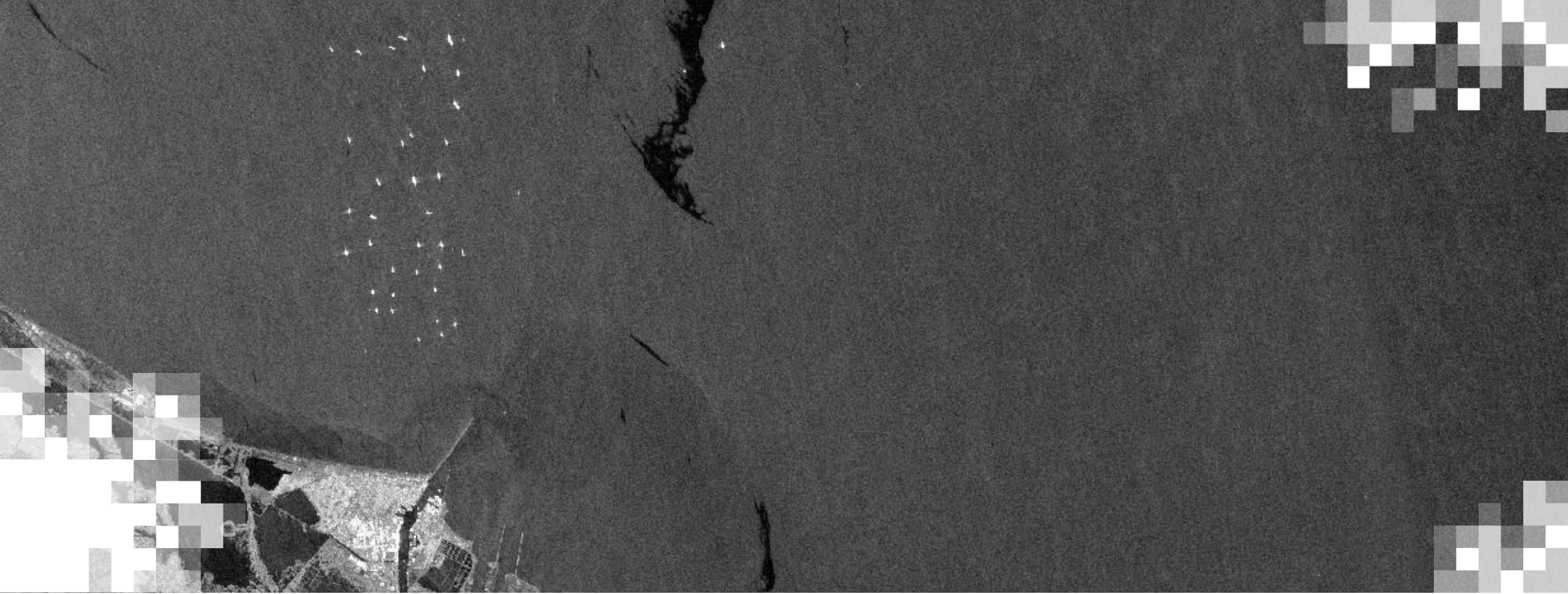
SIR-C L- and C-band Interferometry

- 6-month time separated observations to form interferograms
- Simultaneous C and L band



InSAR experiments have shown good correlation at L-band.

Rosen, P. A., S. Hensley, H. A. Zebker, F. H. Webb, and E. J. Fielding (1996). Surface deformation and coherence measurements of Kilauea Volcano, Hawaii, from SIR-C radar interferometry, *Journal of Geophysical Research* 101, no. E10, 23109-23125, doi:10.1029/96JE01459.



SAR Data for Landslides

SAR Satellites

SAR Satellites	Operational	Repeat Cycle (days)	Wavelength (cm)
European ERS-1 ERS-2	1992 – 2000 1995–2001 (–2011 limited)	35 (1, 3, 183)	6
Canadian Radarsat-1	1995-2013	24	6
European Envisat	2003 – Sep 2010 Oct 2010 – Apr 2012	35 30	6
Japanese ALOS	Jan 2006 – Apr 2011	46	24
German Terra SAR-X TanDEM-X	2007 – present 2010 – present	11	3
Italian COSMO-SkyMed constellation	2007 – present	16 (1, 4, 7, 8)	3
Canadian Radarsat-2	Dec 2007 - present	24	6



New SAR Spacecraft

Satellites (launched or planned)	Repeat Cycle (days)	Wavelength (cm)
European Sentinel-1 (A: Apr 2014, B: May 2015)	A: 12, B: 6	6
Japanese ALOS-2 (May 2014)	14	24
Indian RISAT-1 (Apr 2012)	25	6
NASA-ISRO SAR (NISAR) Mission (Jan 2024)	12	12, 24



NASA-ISRO SAR Mission (NISAR)



- High spatial resolution with frequent revisit time
- Planned launch date: Jan. 2024
- Dual frequency L- and S-band SAR
 - L-band SAR from NASA and S-band SAR from ISRO
- 3 years science operations (5+ years consumables)
- All science data will be made available free and open
- <https://nisar.jpl.nasa.gov>

NISAR Characteristic:	Would Enable:
L-band (24 cm wavelength)	Low temporal decorrelation and foliage penetration
S-band (12 cm wavelength)	Sensitivity to light vegetation
SweepSAR technique with Imaging Swath >240 km	Global data collection
Polarimetry (Single/Dual/Quad)	Surface characterization and biomass estimation
12-day exact repeat	Rapid Sampling
3-10 meters mode-dependent SAR resolution	Small-scale observations
3 years since operations (5 years consumables)	Time-series analysis
Pointing control < 273 arcseconds	Deformation interferometry
Orbit control < 500 meters	Deformation interferometry
>30% observation duty cycle	Complete land/ice coverage
Left/Right pointing capability	Polar coverage, North and South
Noise Equivalent Sigma Zero ≤ -23 db	Surface characterization of smooth surfaces

Slide courtesy of Paul Rosen (JPL)





InSAR Examples: Landslides in California

Slow-Moving Landslides



Slow-moving and
+ catastrophic

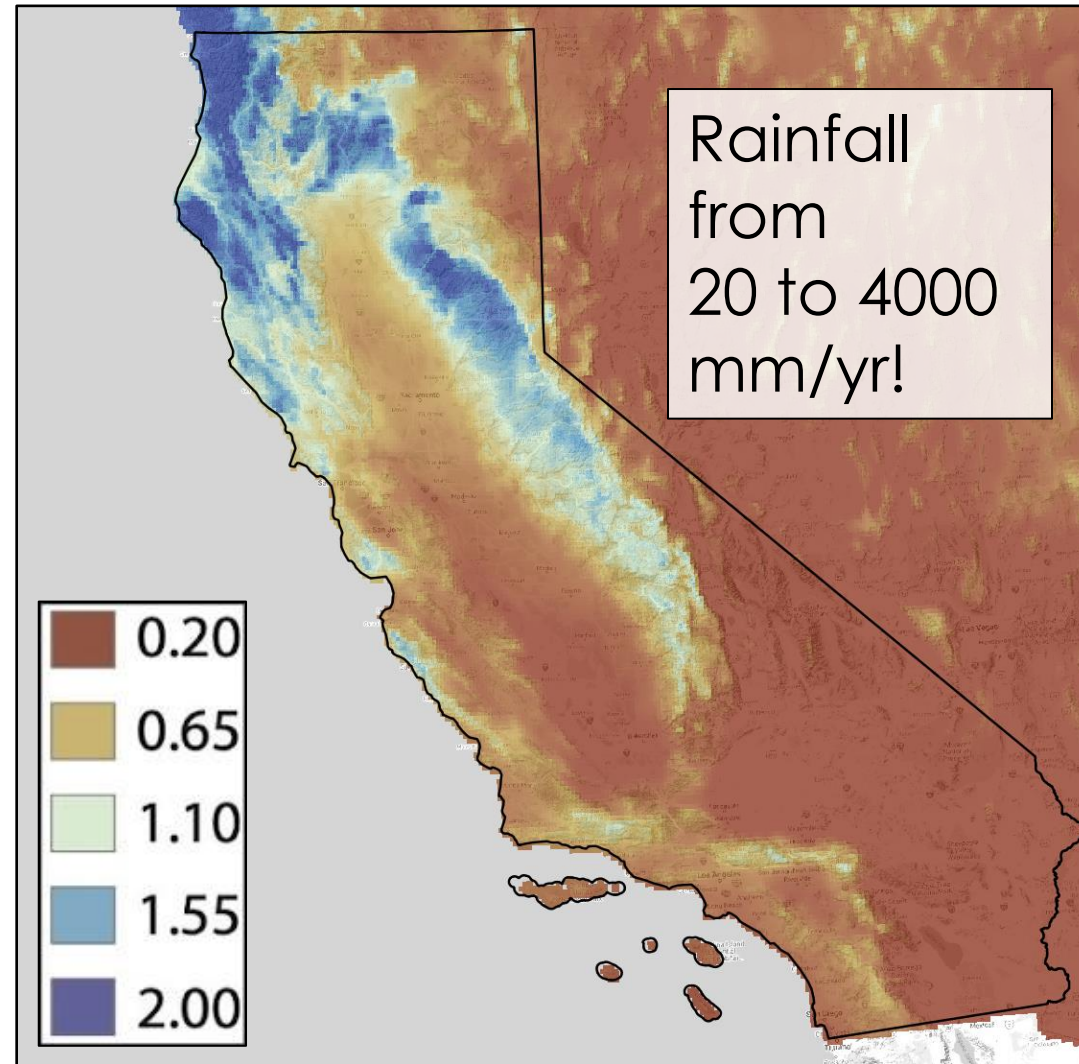


Slow-moving



California Precipitation Variations

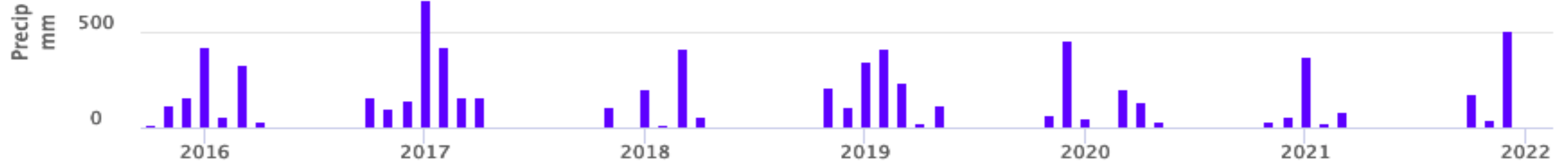
Precipitation (m/yr)



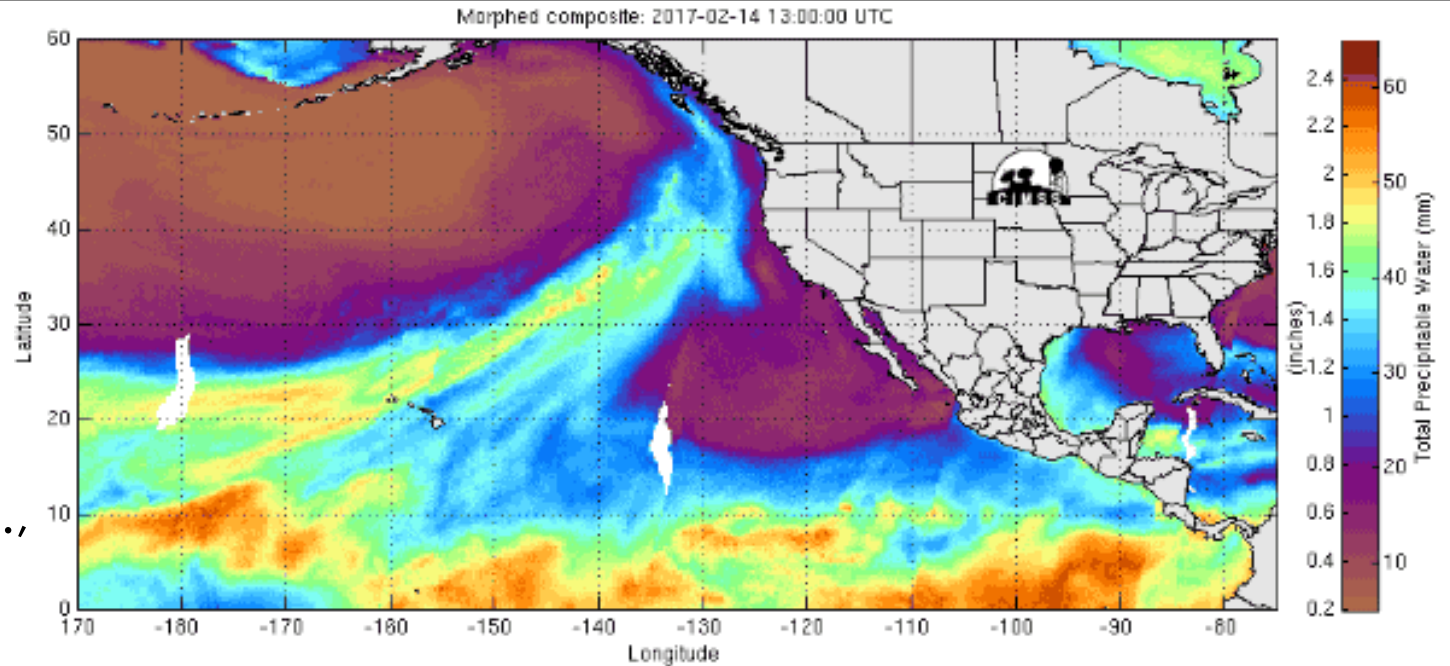
Seasonal and Interannual Precipitation Variations

Big Sur, CA rainfall

Data from PRISM



- Mediterranean climate with seasonal rainfall between Oct – May each year.
- Large changes in rainfall driven in part by atmospheric rivers.
- 30-50% of rainfall in California is delivered by landfalling atmospheric rivers (Dettinger et al., 2011).

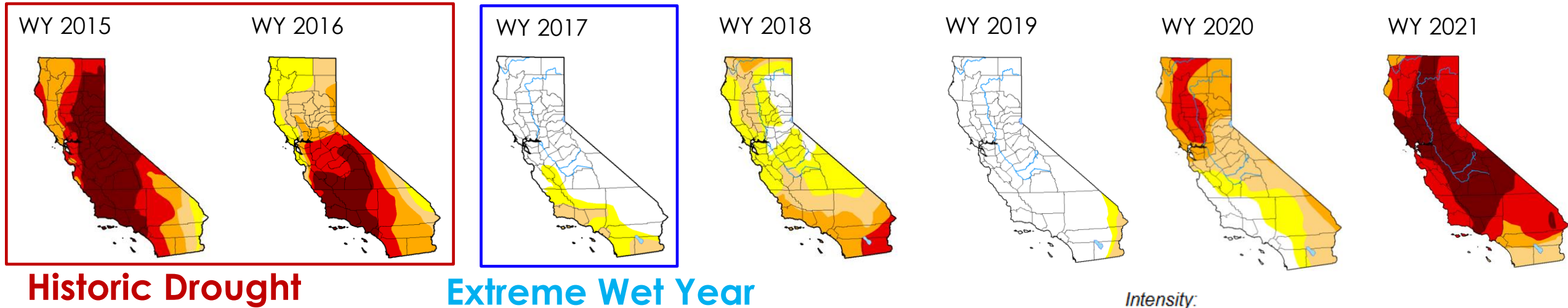


<https://phys.org/news/2017-02-atmospheric-rivers-thought.html>



Interannual Variations

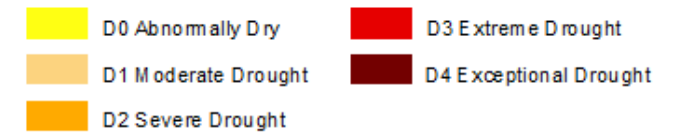
Drought maps of California



Water year (WY) = Oct. 1 - Sep. 30

E.g., WY 2015 = Oct. 1, 2014 – Sep. 30, 2015

Intensity:



The Drought Monitor focuses on broad-scale conditions. Local conditions may vary. See accompanying text summary for forecast statements.

Author:

*Richard Tinker
CPC/NOAA/NWS/NCEP*



Landslide Mapping Methods

SAR Data

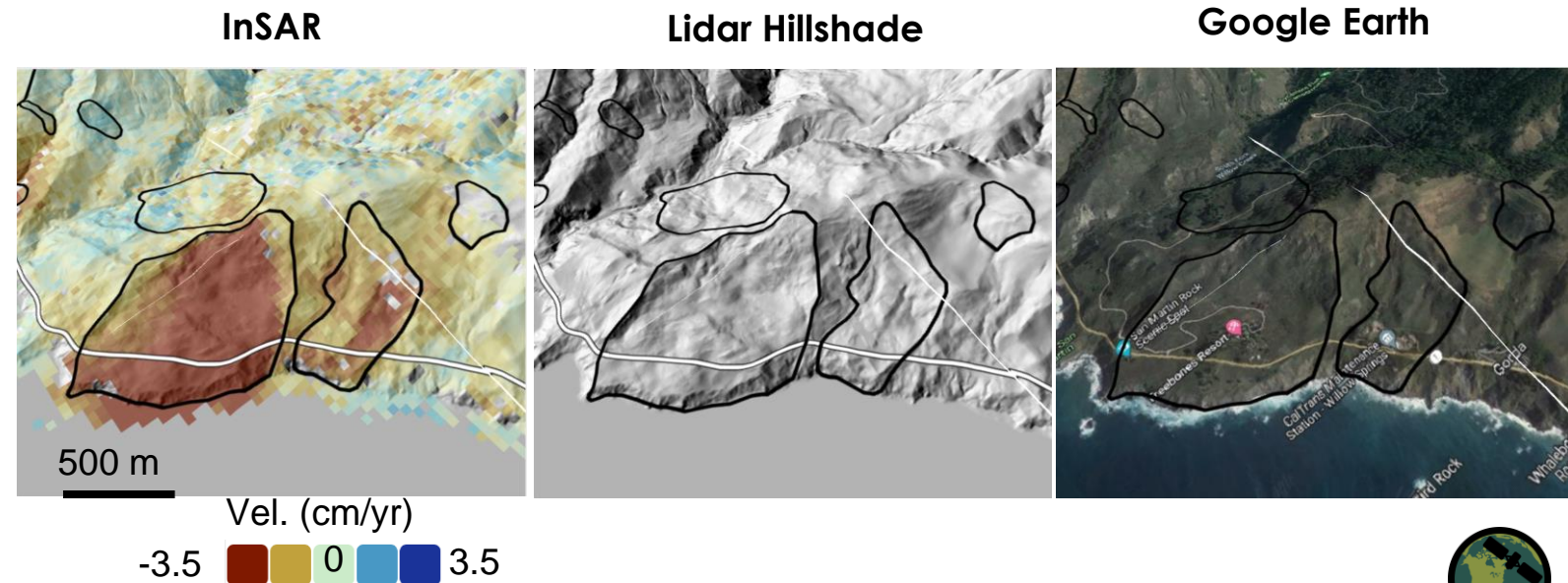
- **Airborne (2009 – today)**
 - NASA/JPL UAVSAR (L-band), *high spatial resolution (~1 m pixels)*
 - ~ 2-4 acquisitions per year
- **Satellites (2015 – today)**
 - Copernicus Sentinel-1 A/B (C-band)
 - New images every 6-12 days
 - 2.5 m x 14 m pixels

To Map Landslides

- Optical imagery and DEMs to confirm landslides
- QGIS

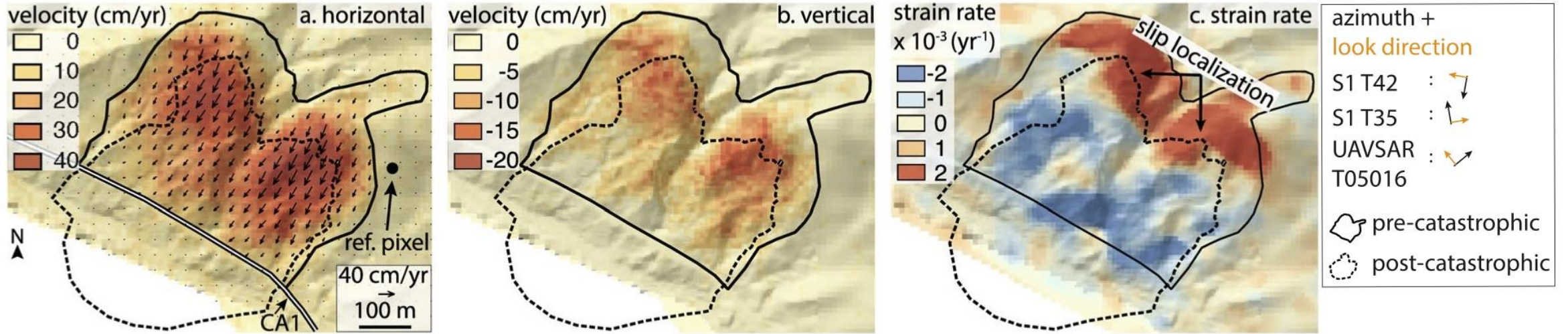
SAR Processing and Analyses

- JPL/Caltech InSAR Scientific Computing Environment (ISCE) (Rosen et al., 2012)
- Miami InSAR Time-series software in PYthon (MintPy) (Yunjun et al., 2019)



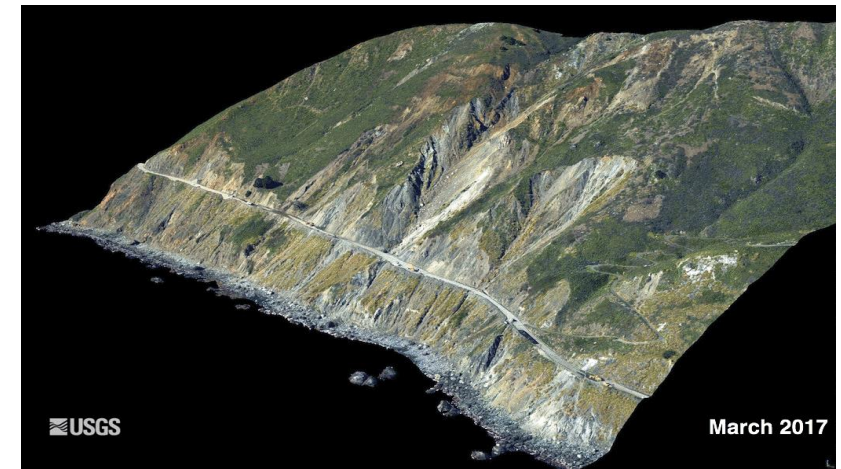
Central California Landslides—Mud Creek

Average velocity and strain rate (2009 - 2017) of Mud Creek landslide, CA



Mud Creek landslide

- Failed catastrophically on May 20, 2017
- Repair cost ~\$54 million
- Sentinel-1 and UAVSAR data combined for 3D displacement

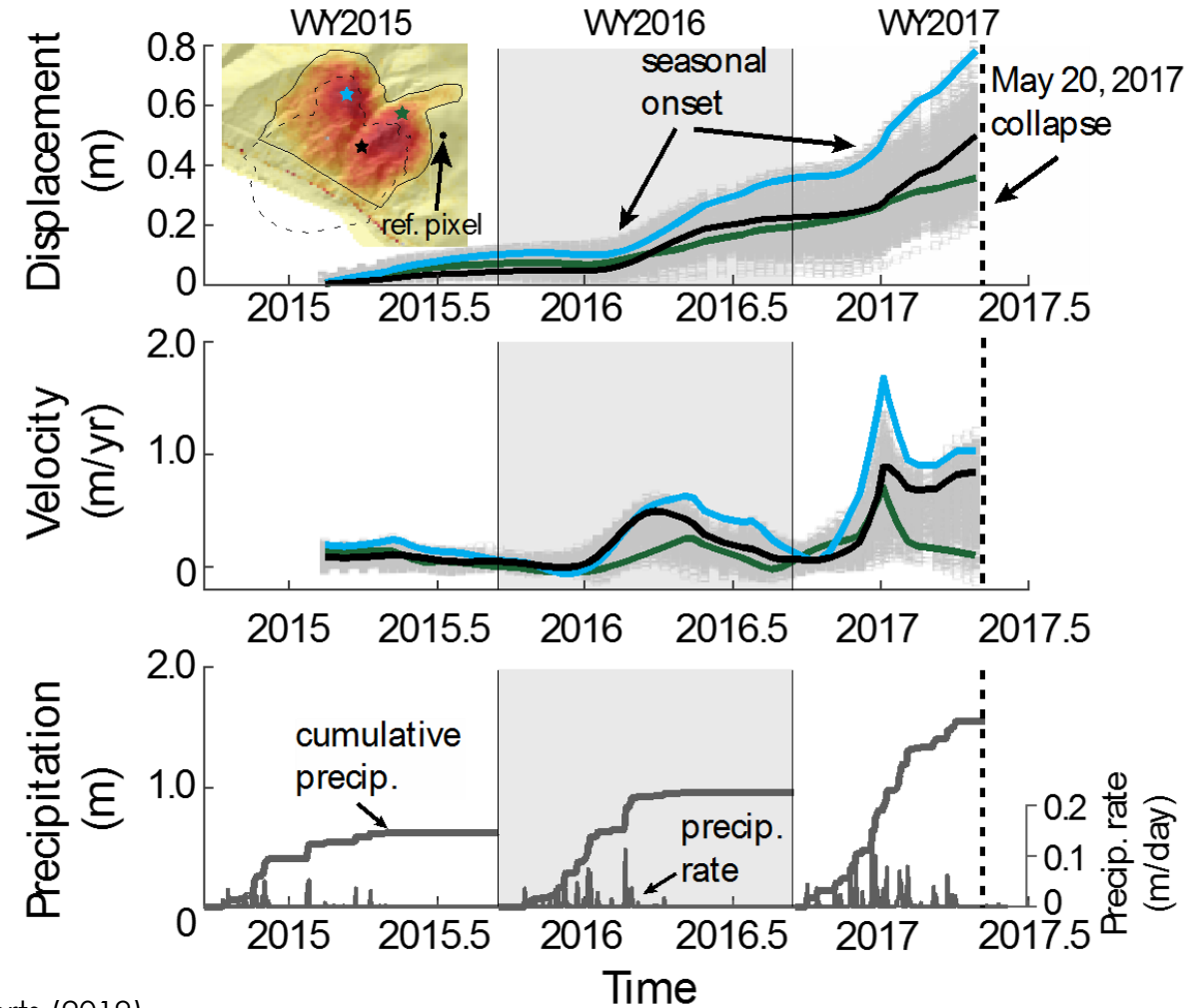
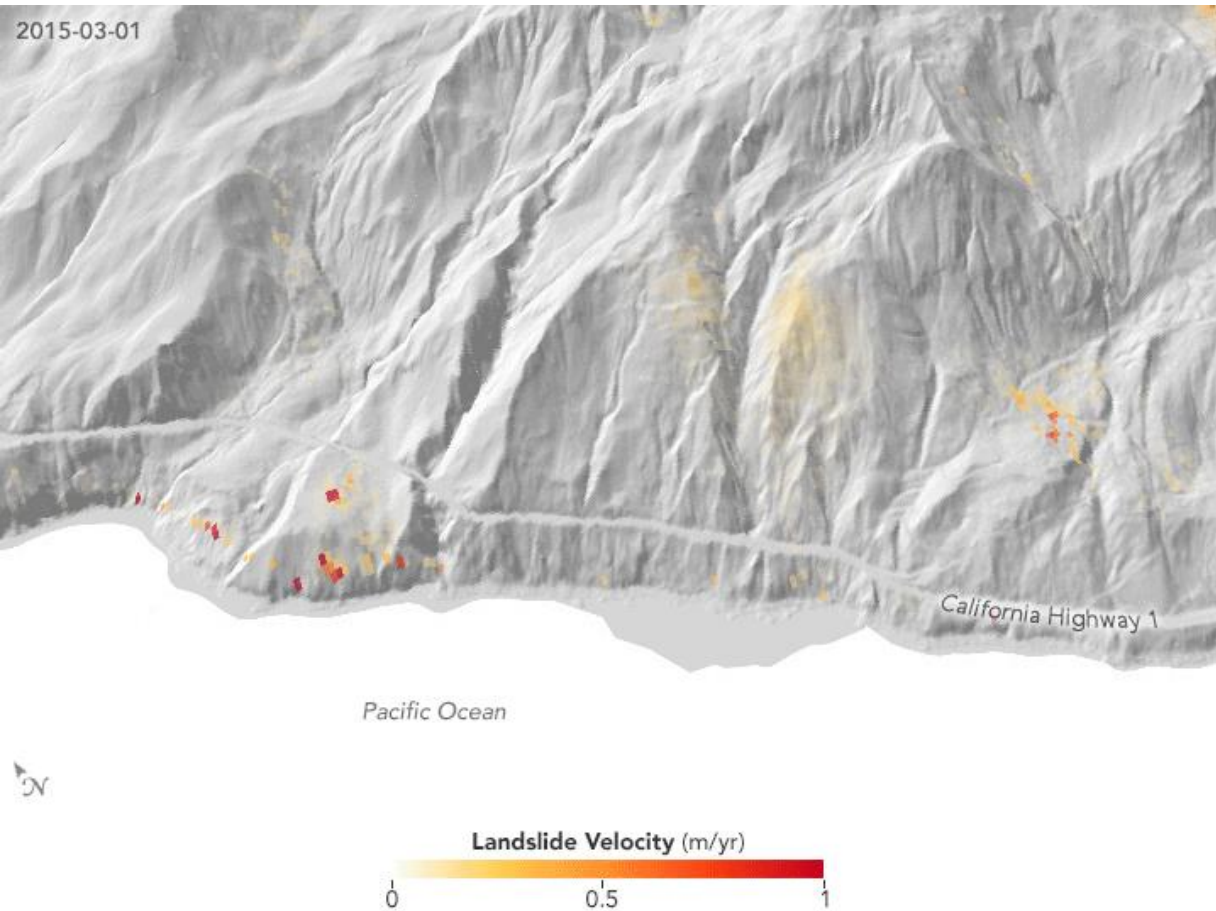


Top: Handwerger et al., Scientific Reports (2019); Bottom: Warrick et al. 2019, <https://walrus.wr.usgs.gov/remote-sensing/>



Mud Creek Landslide Time Series

Mud Creek Landslide



(Left) InSAR Time Series from Sentinel 1; (Right) Handwerger et al., Scientific Reports (2019)

Handwerger, A. L., M.-H. Huang, E. J. Fielding, A. M. Booth, and R. Bürgmann (2019). A shift from drought to extreme rainfall drives a stable landslide to catastrophic failure, Scientific Reports 9, no. 1, 1569, doi:10.1038/s41598-018-38300-0.



Preprocessed Interferograms

JPL/Caltech Advanced Rapid Imaging and Analysis (ARIA) InSAR Standard Product—Getting Ready for NISAR

- Use InSAR standard products to identify and monitor landslides over massive regions
- Sentinel-1 SAR data 2015-2021 processed to geocoded unwrapped (GUNW) interferograms with ~90 m pixel spacing – better for larger landslides!



[ARIA-tools-docs](#)

python 3.5+ license GPL

download, merge,
and prepare data
for time series

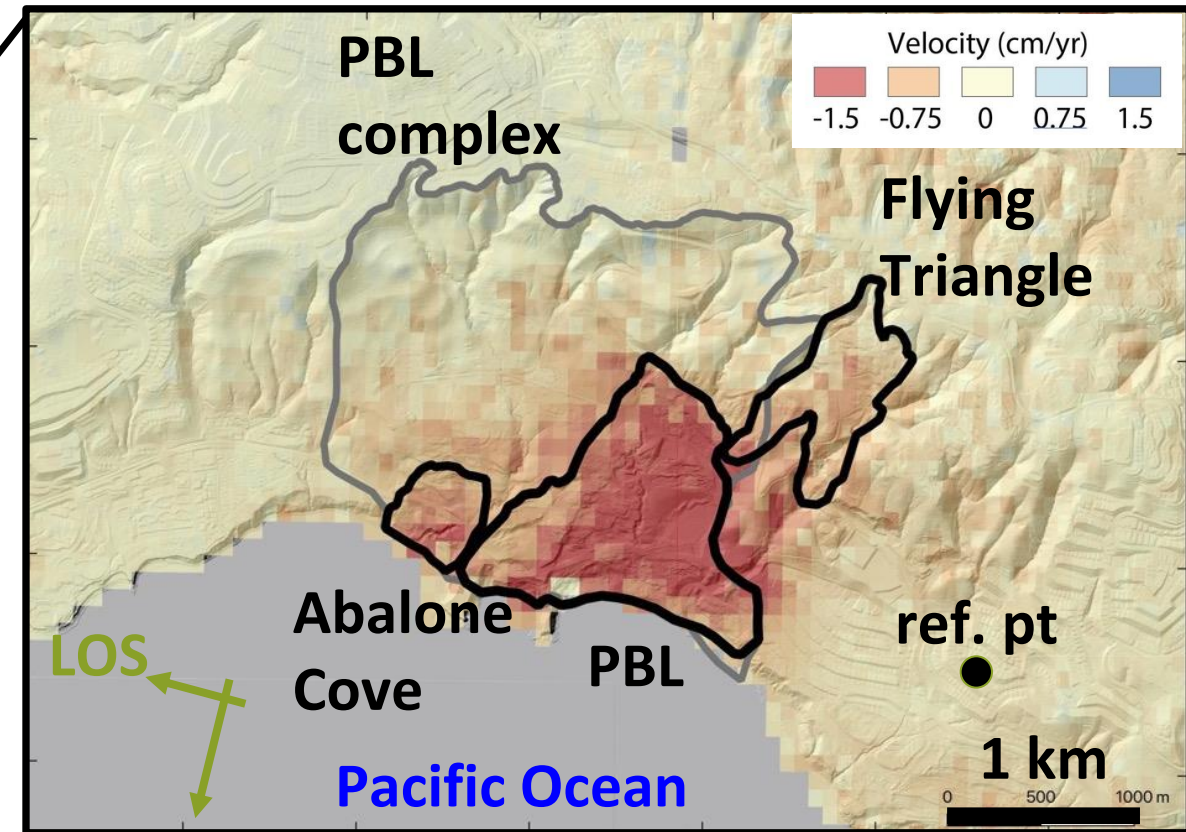
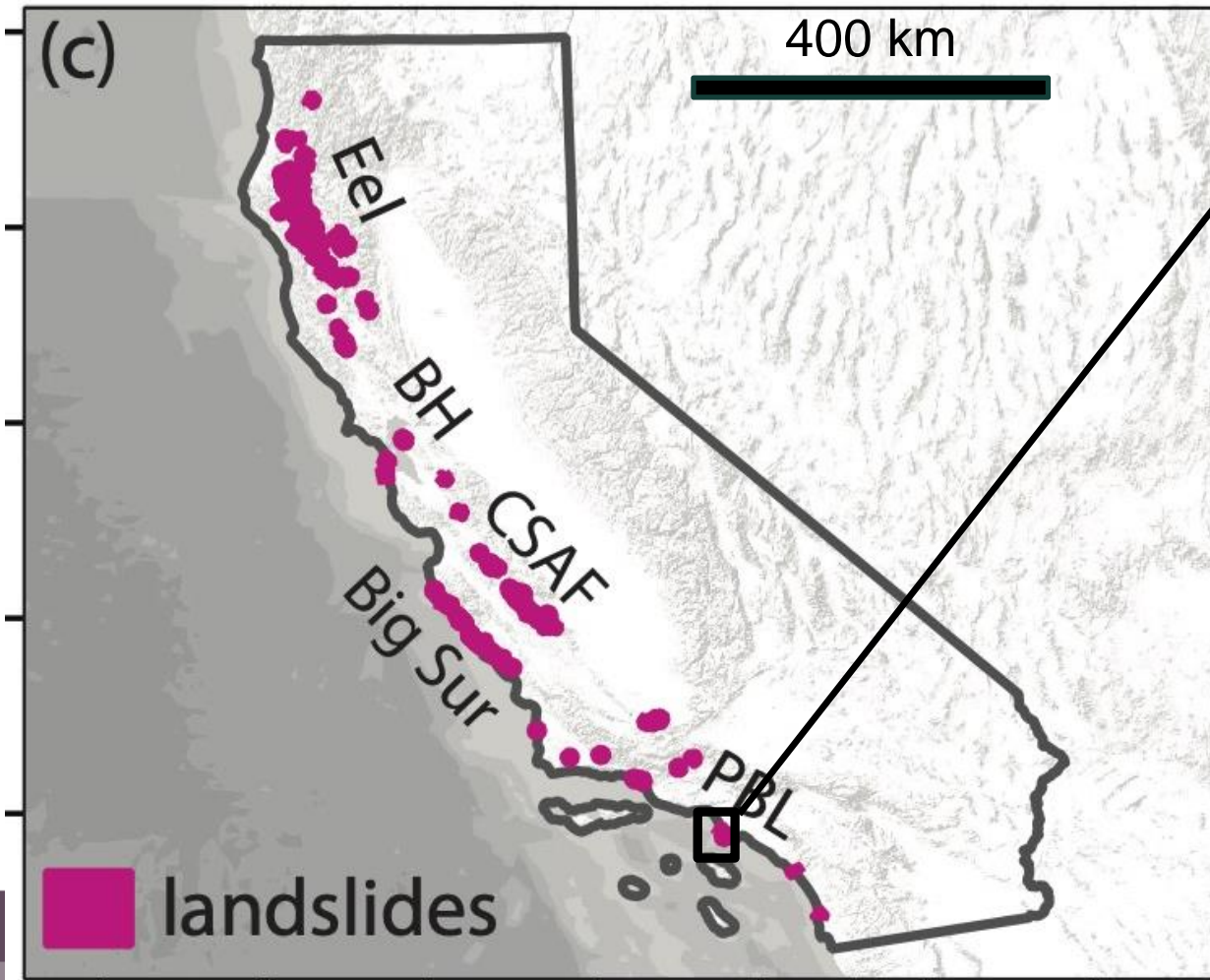
<https://github.com/aria-tools/ARIA-tools-docs>



California Landslide Map from InSAR

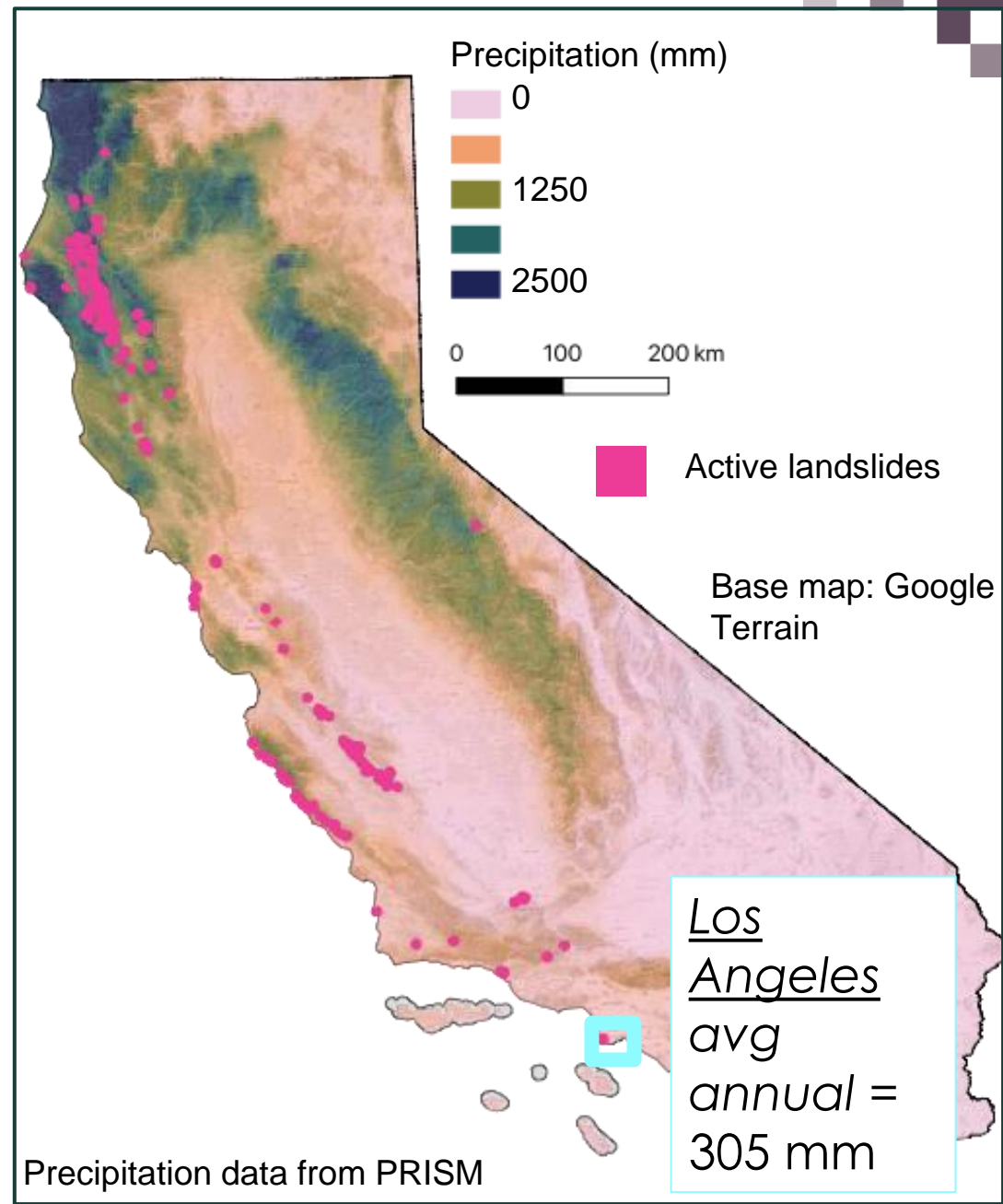
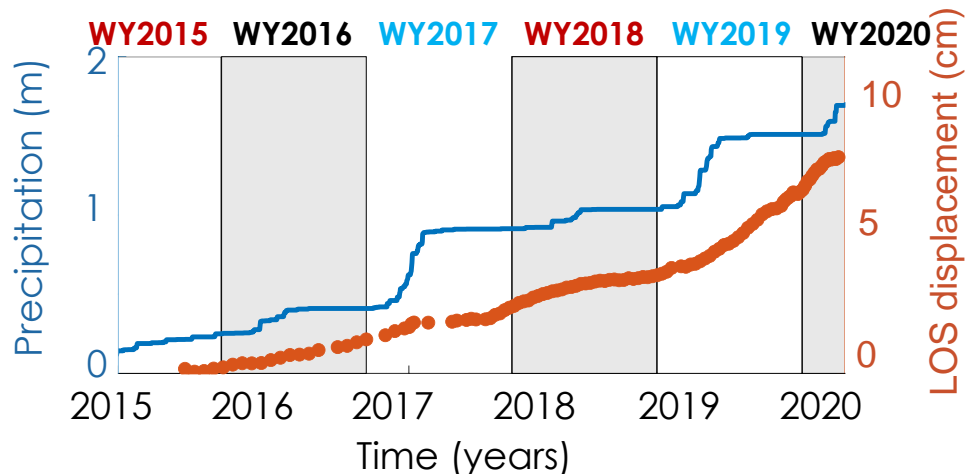
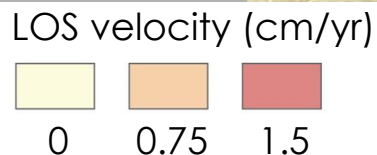
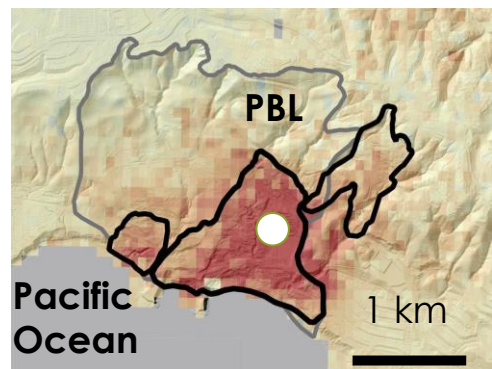
Landslide Inventory 2015-2020

- We have identified 247 active landslides
- ARIA standard product best suited for larger landslides that exhibit persistent motion

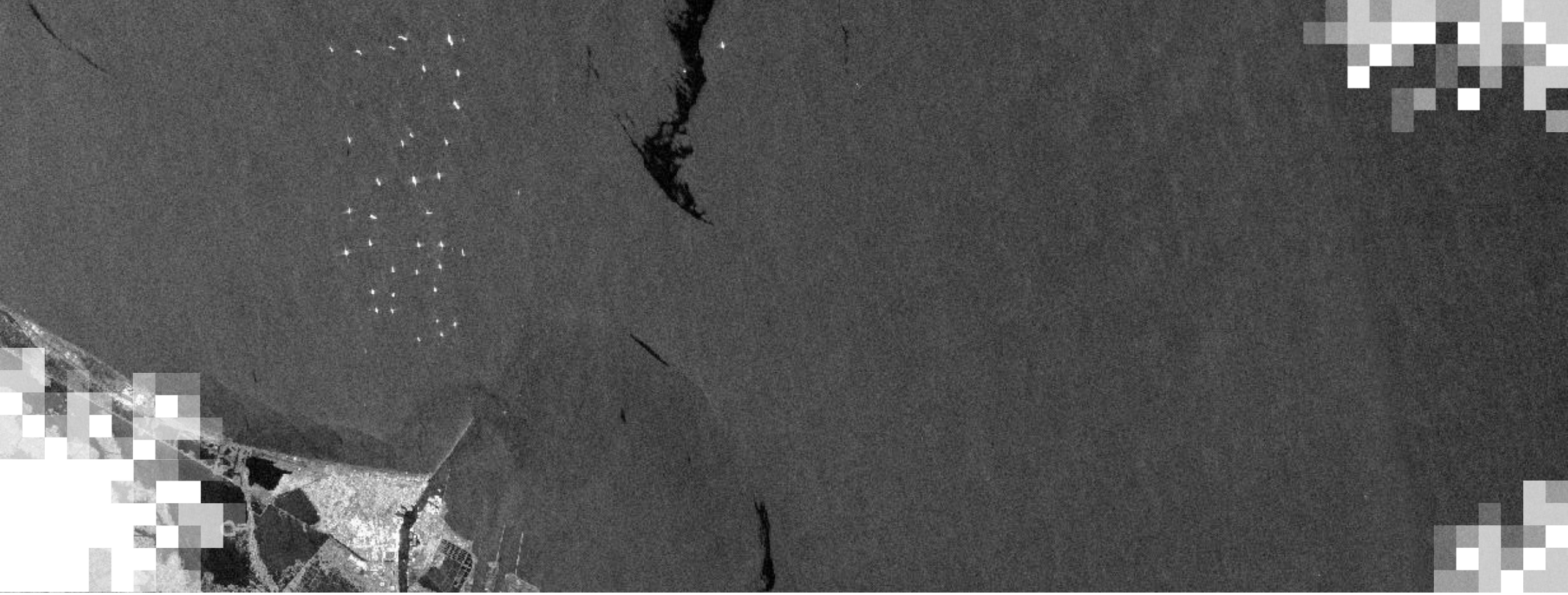


Landslide Velocity Time Series

Portuguese Bend landslide, Los Angeles, southern California



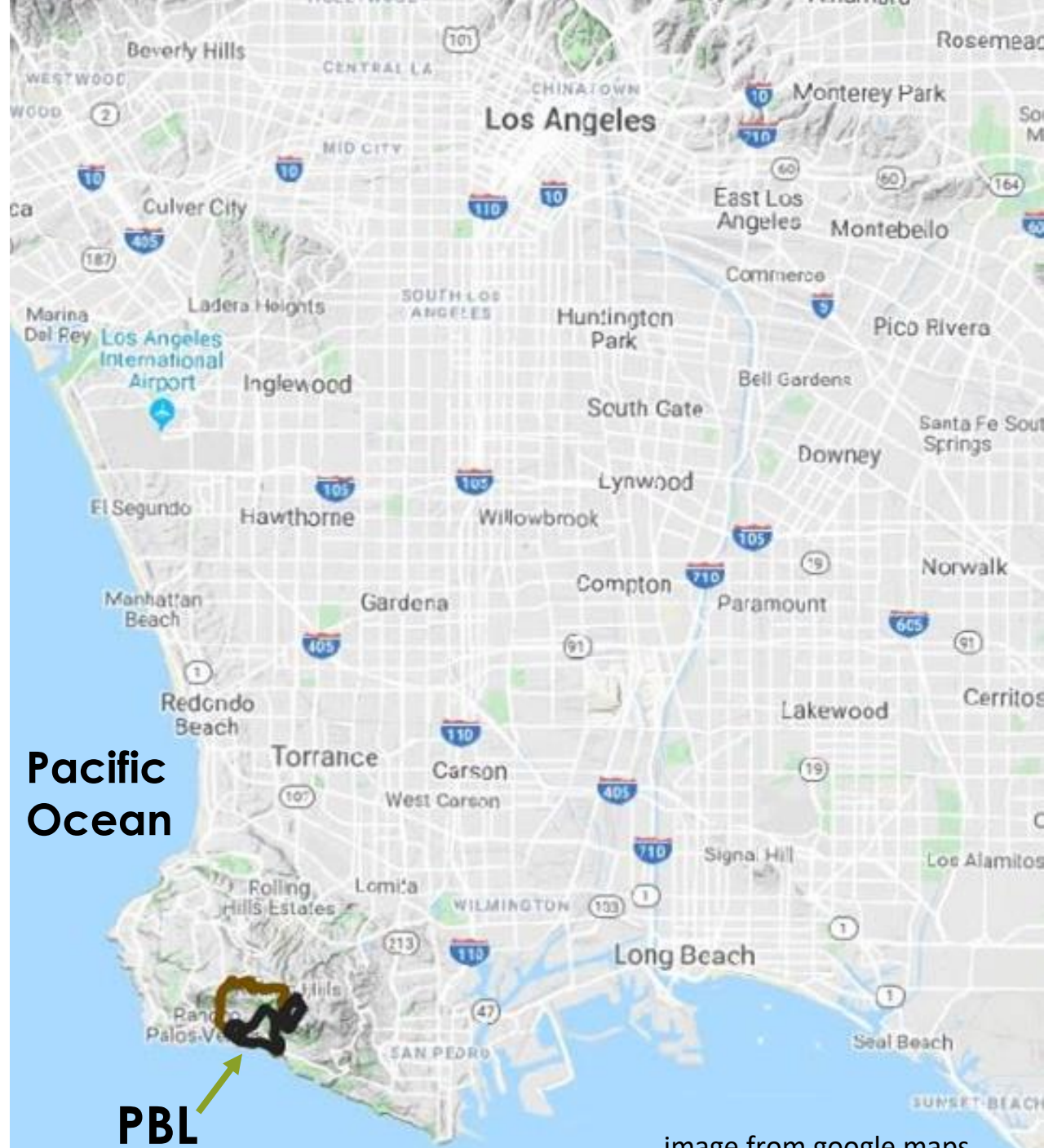
Handwerger, A. L., E. J. Fielding, S. S. Sangha, and D. P. S. Bekaert (2022). Landslide Sensitivity and Response to Precipitation Changes in Wet and Dry Climates, *Geophysical Research Letters* 49, no. 13, doi:10.1029/2022gl099499.



Portuguese Bend Landslide

Portuguese Bend Background

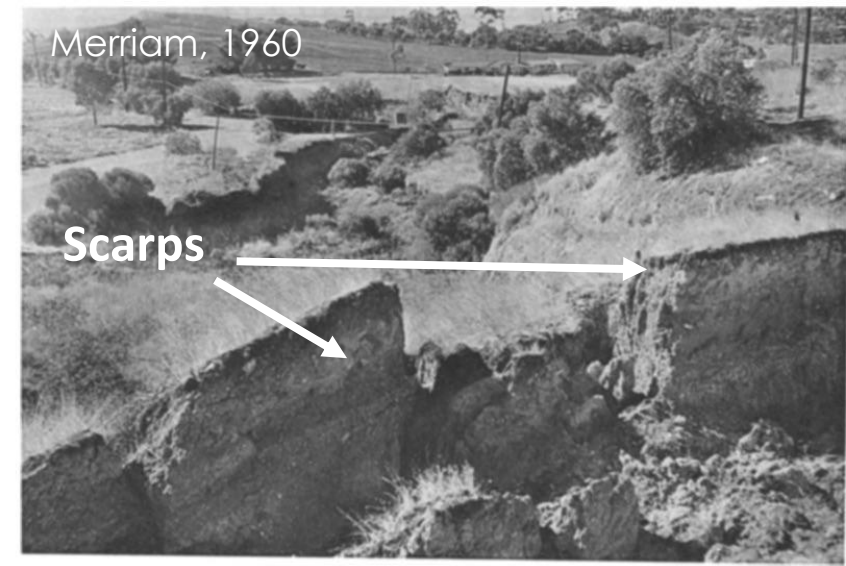
- The Portuguese Bend Landslide (PBL) is an active slow-moving landslide located on the Palos Verdes peninsula, Rancho Palos Verdes, Los Angeles County, CA.
- The PBL has been active since 1955.
- Reactivated by surface loading during construction during the planned extension of Crenshaw Boulevard (Merriam, 1960).



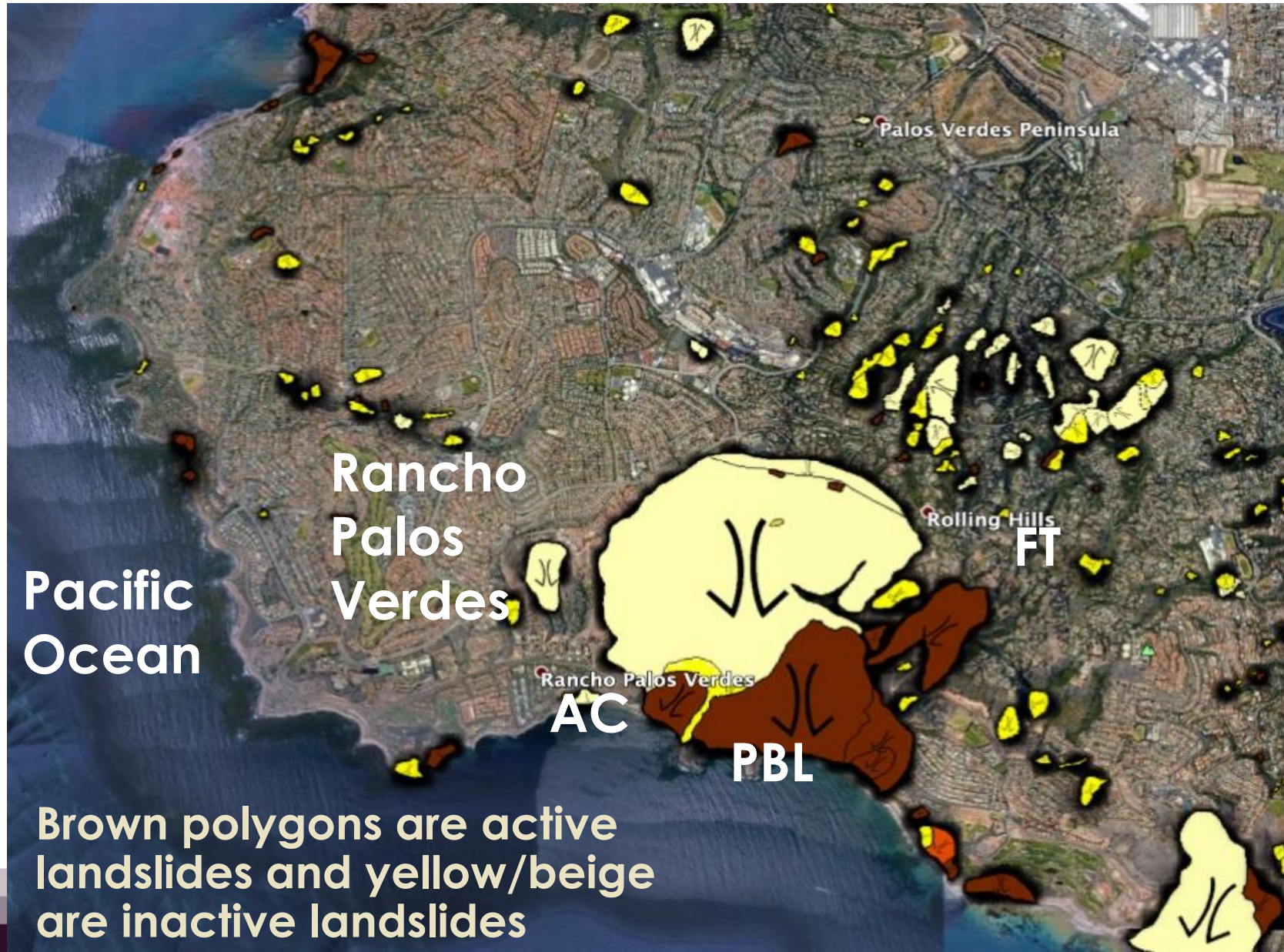
PBL Impacts

Hazardous impact (overview by Stephens & Associates, Inc, 2018)

- major damage to infrastructure that is still ongoing ...
 - 140 homes have been displaced or destroyed
 - \$50 million spent by City of Rancho Palos Verdes for repairs
- There have been major efforts to stop the landslide including:
 - groundwater drainage
 - diverting stormwater
 - reinforced concrete “shear pins”
 - regrading
 - surface infiltration control
 - above ground piping



Landslide Activity on Palos Verdes

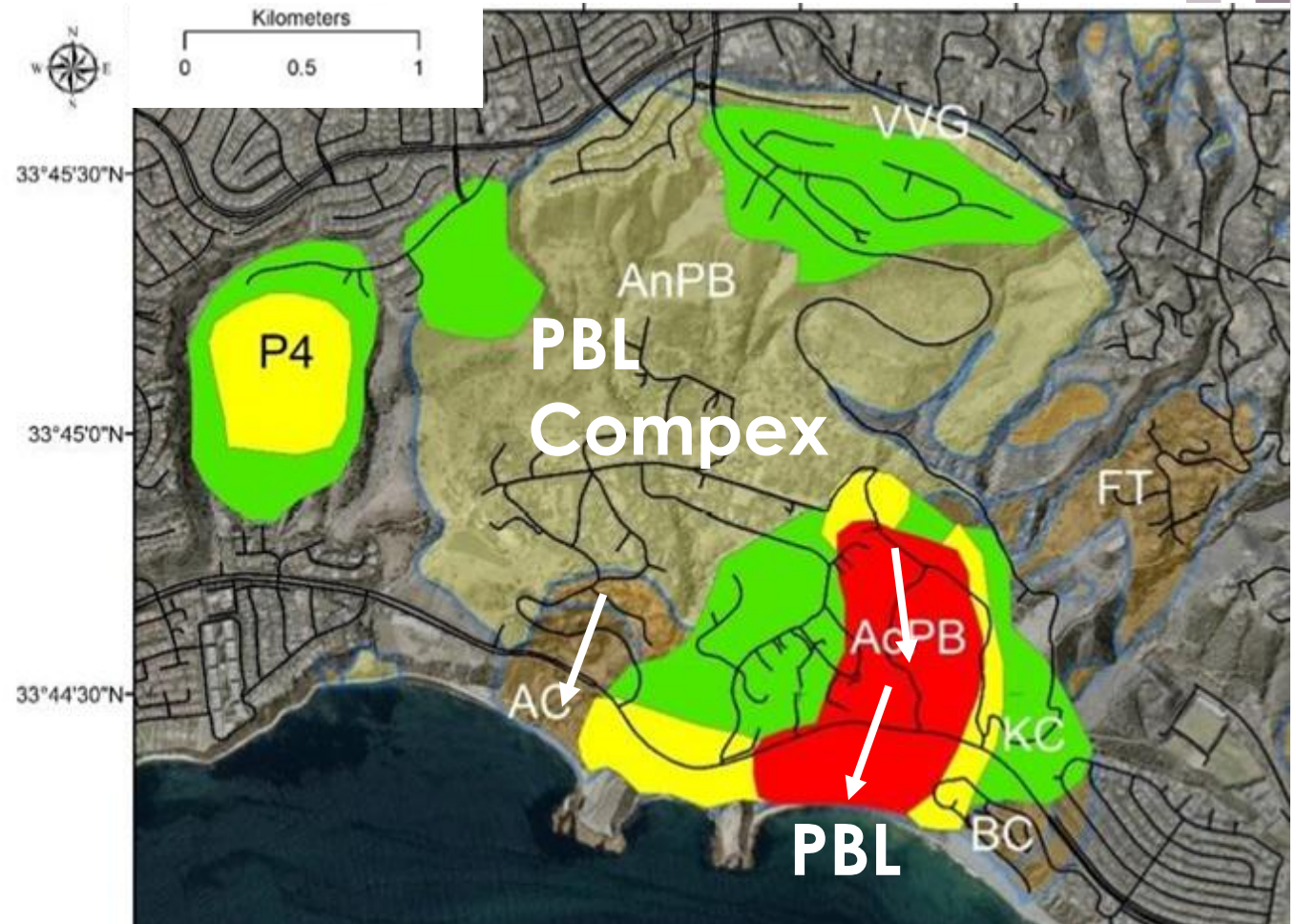


- California State Geologic Survey (CGS) landslide inventory shows many landslides on the Palos Verdes peninsula (Haydon, 2007).
- Palos Verdes is densely populated, except for the PBL complex!



PBL Complex

- Active landslide has an area = 1.25 km^2 and thickness = 5 to 75 m
- Kinematics vary in space and time
- Between 1956 - 2002 the landslide moved $\sim 150 \text{ m}$ with an avg. rate of $\sim 3.5 \text{ m/yr}$ (Kayen et al., 2002)
- Between 2007-2017 the landslide moved $\sim 20 \text{ m}$ with an avg rate 1-2 m/yr (Bouali et al., 2019)



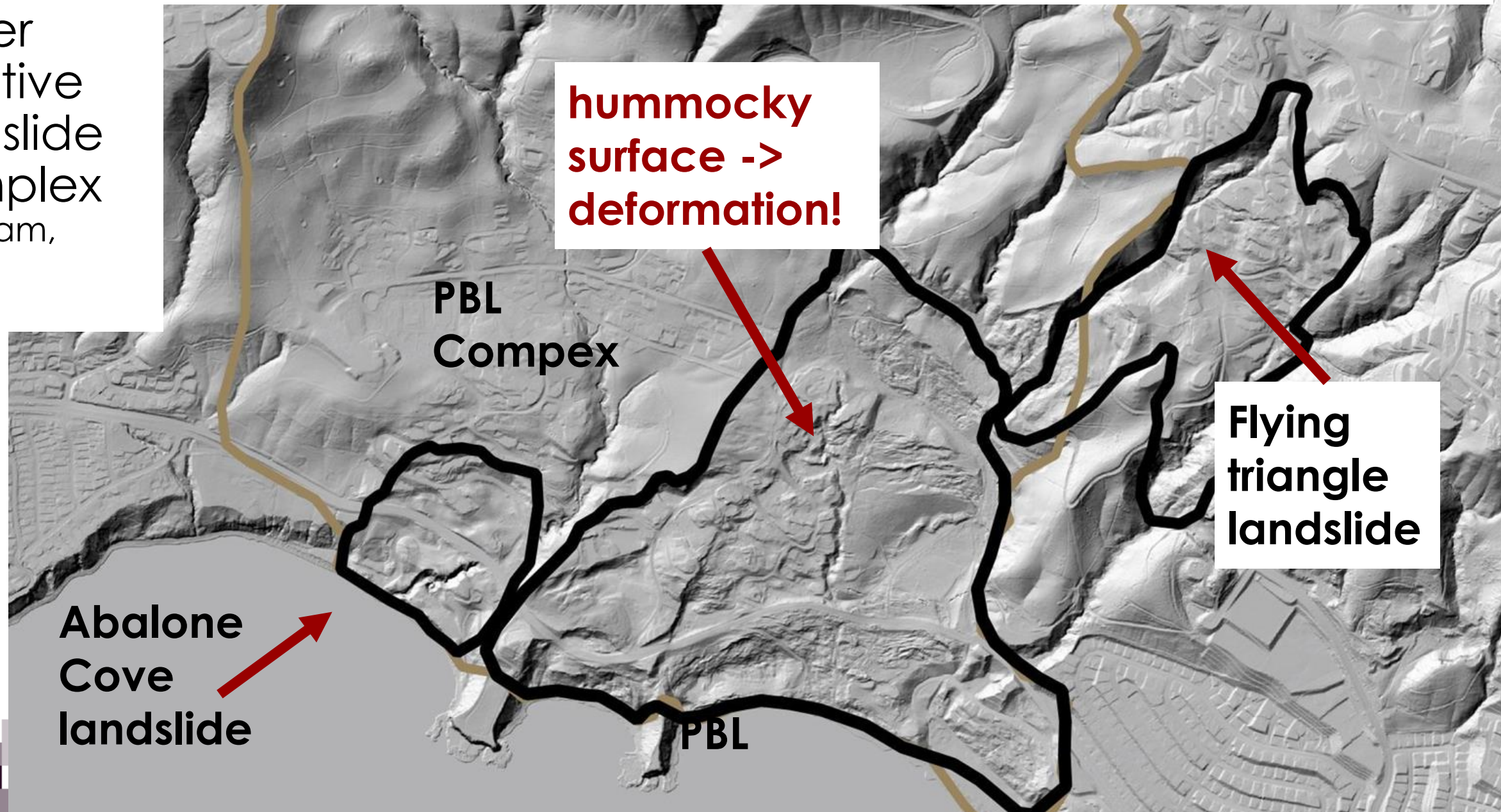
Landslide Activity	Slow Landslides	Very Slow Landslides	Extremely Slow Landslides
	1.5 to 18 m/yr	60 mm/yr to 1.5 m/yr	< 60 mm/yr

Bouali et al. (2019)



The PBL is part of a larger inactive landslide complex (Merriam, 1960)

USGS Lidar Hillshade



hummocky surface -> deformation!

PBL Complex

Flying triangle landslide

Abalone Cove landslide

PBL

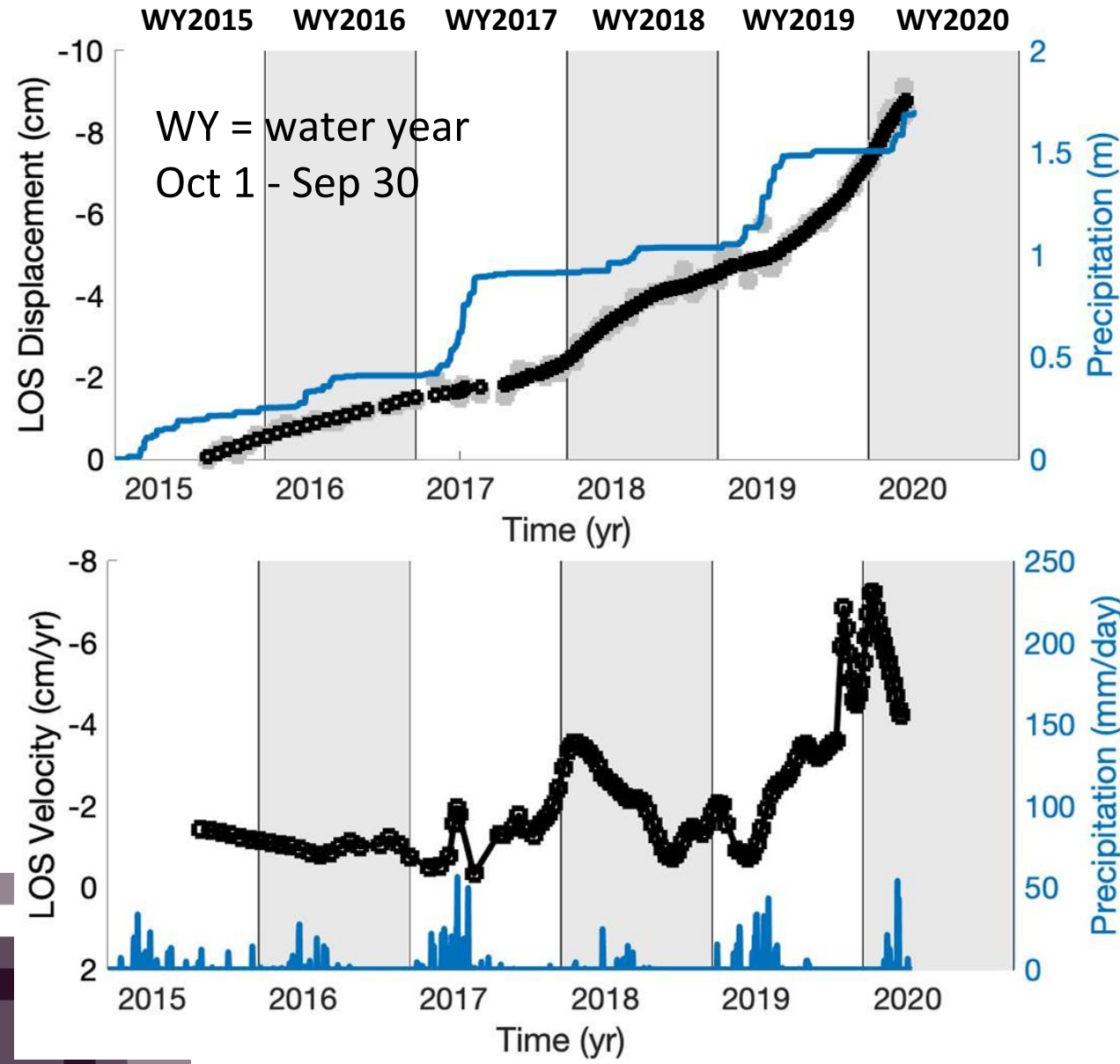
Methods

ARIA-tools and MintPy

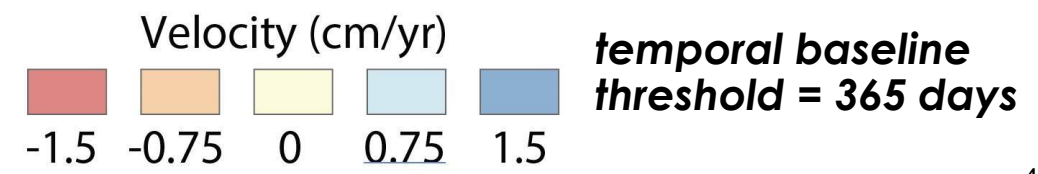
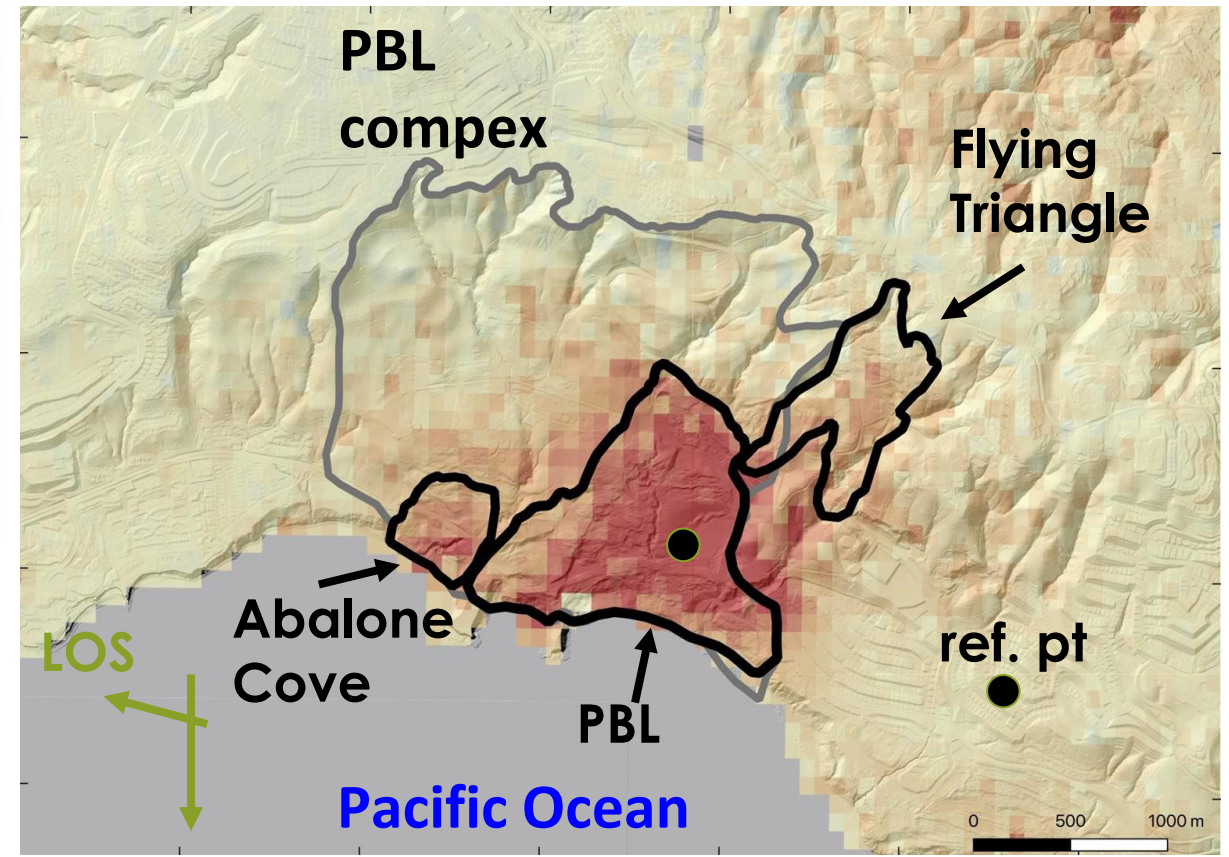
- To quantify the landslide deformation between 2015 and 2020, we used pre-processed InSAR from Copernicus Sentinel-1 (S1) satellites that was processed automatically with the ARIA system (Bekaert et al., 2019).
- ARIA-tools-docs (<https://github.com/aria-tools/ARIA-tools-docs>) describe usage of ARIA-tools to read the ARIA products.
- The time-series analysis is done with MintPy (Yunjun et al., 2019) (<https://github.com/insarlab/MintPy>)

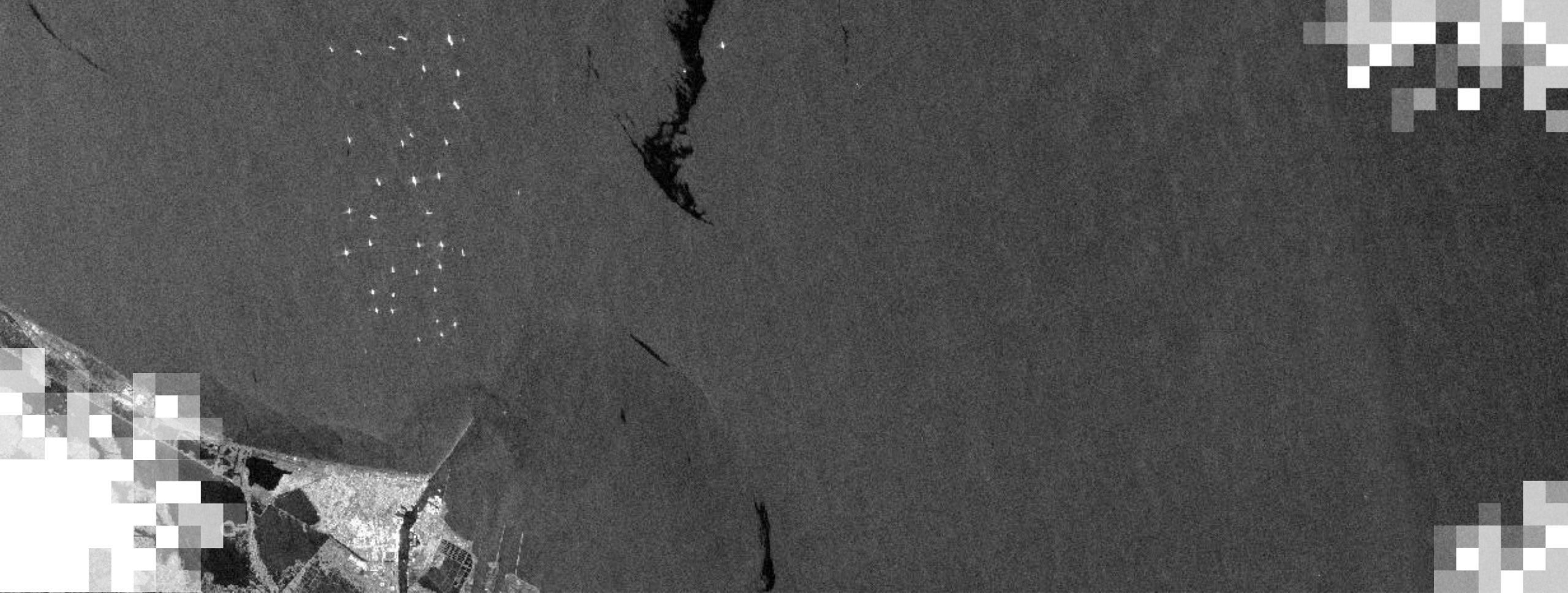


Results - T71d Time Series



T71d - Avg. linear velocity 2015-2020





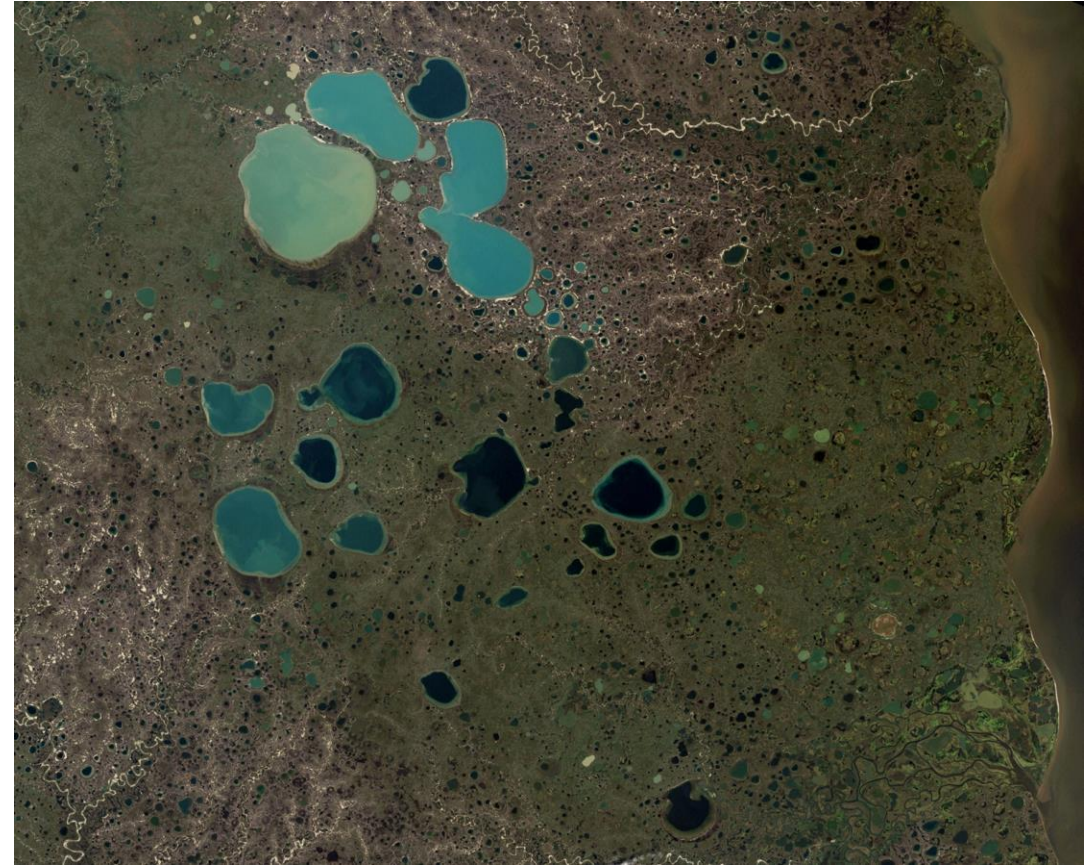
Accessing, Opening, and Displaying SAR Interferometry Time Series Data

Data Processing Demonstration

The steps of the data processing with ARIA-tools and MintPy are in the Jupyter notebook.

Questions?

- Please enter your questions in the Q&A box. We will answer them in the order they were received.
- We will post the Q&A to the training website following the conclusion of this session.



<https://earthobservatory.nasa.gov/images/6034/pothole-lakes-in-siberia>



Contacts

- Trainer:
 - Eric Fielding: eric.j.fielding@jpl.nasa.gov
- Training Webpage:
 - <https://appliedsciences.nasa.gov/join-mission/training/english/arset-disaster-assessment-using-synthetic-aperture-radar>
- ARSET Website:
 - <https://appliedsciences.nasa.gov/arset>
- Twitter: [@NASAARSET](https://twitter.com/NASAARSET)





Thank You!

